Self-healing of steel corrosion in a model alkaline medium: electrochemical response and surface analysis

D. A. Koleva[1], J. Hu[2], H. Kolev[3], K. & Van Breugel[1]
[1]Department of Materials and Environment,
Faculty of Civil Engineering and Geosciences,
Delft University of Technology, The Netherlands
[2]School of Materials Science and Engineering,
South China University of Technology, P.R. China
[3]Bulgarian Academy of Sciences, Institute of Catalysis, Sofia, Bulgaria

Abstract

The application of polymeric nano-particles for corrosion control in reinforced cement-based systems was studied. As an initial investigation, steel electrodes (St37) were tested in modified cement extract (CE), which is a model pore solution of pH 12.9 and chemical composition: 201 mg/l Ca; 3.85 mg/l K; 1.33 mg/l Na; 4 mg/l Al, Fe < 1 mg/l. Corrosion initiating factor was 5% NaCl. PEO_{113}-b-PS_{780} vesicles at 0.0024 wt.% in the CE were employed. These are nano sacs of 220 nm, enclosing a volume with a thin membrane, thus able to effectively entrap water-soluble compounds. Ion binding (bulk liquid medium), steel surface adsorption and/or participation in oxide layers formation were the expected mechanisms of particles' involvement. Both "empty" and "Ca-containing" vesicles were studied to evaluate "barrier" effects only vs. self-healing mechanisms. Increased steel corrosion resistance in the presence of both vesicle types was observed, however, it was more pronounced when Ca-containing ones were involved. CVA and XPS analysis, substantiate the self-healing phenomena, through a direct evidence of pitting formation and propagation and consecutive healing (and no further pit formation) when Ca-containing vesicles are present.
Keywords: corrosion, cement extract, vesicles, self-healing.

1   Introduction

The alkaline nature of concrete (pH=12.6-13.5) generally provides a physicochemical barrier against corrosion of the embedded steel and assures the formation of a stable passive layer on the steel surface [1]. However, corrosion is initiated due to carbonation (pH drop < 9) or chloride contamination (pH drop < 5) [2–8], resulting in corrosion propagation, accelerated damage and rapid failure [9]. Various protection methods and techniques have been investigated and are successfully applied, e.g. protective coatings/sealers [10, 11]; polymer coatings and cathodic protection (CP) (the latter combination leading to increased current demand/de-bonding [12] and possible hydrogen embrittlement or bond-strength degradation [13–18]); concrete re-alkalization [19]; corrosion inhibitors (quickly exhausted and with none or even negative effects on the bulk cement-based matrix [19–21]). Well known is that each method/technique has its limitations and side effects. Moreover, there is no technique that considers both steel reinforcement and cement-based bulk matrix, aiming at improved properties of both materials and superior global performance of reinforced concrete as a system. To this end, in the frame of a novel approach and (initially) within the IOP Self-Healing project SHM08743, executed in TU Delft and financially supported by Agentschap, NL, tailor-made polymeric nano-materials were studied. The aim was to increase steel corrosion resistance via self-healing of corrosion damage, along with improved microstructural characteristics.

As far as the cement-based bulk matrix properties were concerned, the suggested hybrid core-shell nano-particles already proved their positive effect, for example: in the presence of polyethylene oxide $(PEO)_{113}$-b- polystyrene $(PS)_{218}$ micelles (50 nm size) of only 0.025 wt.% per cement weight, the porosity of the micelle-modified matrix was reduced two times, whereas water permeability was reduced with six orders of magnitude; a more uniform distribution of calcium-silicate-hydrate (C-S-H) and enhanced mechanical properties, but un-disturbed water balance was evident from nano-indentation tests [22–25]. For establishing the effects on corrosion resistance, the aforementioned micelles, as well as stabilized (kinetically frozen) PEO_{113}-b-PS_{760} vesicles (220 nm size), "empty" and Ca-containing ones, were studied [26–28]. The aim of these studies was to investigate the possibility for maintained positive effects on the cement-based microstructure, along with increased corrosion resistance and self-healing (or repair) of corrosion damage, resulting from Ca-core release. Initial tests were performed in model pore solutions, prior to studies in reinforced mortar and concrete. This paper briefly presents some main outcomes from the investigation on corrosion resistance of St37 steel electrodes in cement extract, modified with the above defined vesicles [28]. Further, this work substantiates improved corrosion resistance and evidence of self-healing effects through correlating electrochemical performance and steel surface analysis.

2   Materials

Polymeric vesicles: vesicles were prepared via dialysis from PEO_{113}-b-PS_{760} block-polymer [24–28]. In order to distinguish between "barrier" effects and "self-healing" due to Ca-release, both "empty" and Ca-containing vesicles were used. Their hydrodynamic radius was approximately 220–250 nm, identified by dynamic light scattering (DLS) measurement and transmission electron microscopy (TEM) (Fig. 1).
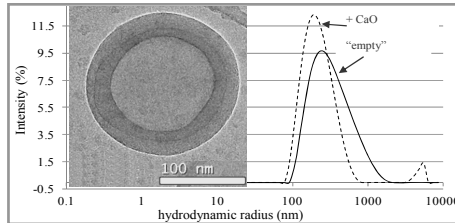

Figure 1:   DLS and TEM of vesicles

Cement extract (CE): as a model pore solution was prepared by mixing Ordinary Portland cement CEM I 42.5N and tap water in 1:1 ratio; after 24h rotation the suspension was filtrated and this solution was used as a model medium. The pH of CE is 12.6–2.9, the chemical composition, derived via Inductive coupled plasma spectrometry (ICP) was: Ca – 201 mg/l; K – 3.85 mg/l; Na – 1.33 mg/l; Al – 4 mg/l and Fe < 1 mg/l; NaCl was corrosion-inducing factor, added in a concentration of 10 g/l to the CE. The aqueous solution of PEO_{113}-b-PS_{760} vesicles was added to CE, thus the vesicles concentration was 0.0024 wt. % in chloride-free and chloride-containing CE.

Steel electrodes: low-carbon steel St37 with surface area of 4 cm^2 was used. All electrodes were equally treated (grinding, polishing, acetone cleaning and water rinsing) prior to treatment in the relevant solutions and electrochemical measurements. Three replicates per condition were tested. Sample designation is as follows: group CE – steel in CE only; CEn – steel in chloride-containing CE; CEV and CEVC stand for steel in CE modified with "empty" and "Ca-containing" vesicles, whereas CEVn and CEVCn stand for the corroding cells respectively.

3   Methods

Electrochemical measurements: Autolab-Potentiostat PGSTAT 30, combined with FRA2 module, using GPES and FRA interface was used. Linear polarization resistance (LPR), Potentio-dynamic polarization (PDP), Impedance spectroscopy (EIS) and Cyclic voltammetry (CVA) were employed, using a common 3-electrode cell arrangement (saturated calomel electrode, SCE, as reference electrode). EIS was performed at open circuit potential (OCP) in the frequency range of 50 kHz to 10 mHz by superimposing an ac voltage of 10 mV; LPR used a polarization window of ± 20 mV vs. OCP; PDP was in the range of

-0.2V to +1.0V vs. OCP at a scan rate 0.5 mV/s; CVA scans were in the potential region of −1.4V to 0.6V at a scan rate of 5 mV/s (all electrochemical measurements are as generally employed for the systems under study [22–27]).

Surface analysis: morphology and composition of the product layers were investigated using scanning electron microscopy (SEM), coupled with energy dispersive X-ray (EDX) analysis as a qualitative and semi quantitative technique, using ESEM Philips XL 30. X-ray photoelectron spectroscopy (XPS) was carried out in the UHV chamber of an electron spectrometer ESCALAB-MkII VG Scientific with a base pressure of about 1×10^{-10} mbar (during the measurement 1×10^{-9} mbar). The photoelectron spectra were obtained using unmonochromatized Al Kα (hν = 1486.6 eV) radiation. Passing through 6 mm slit (entrance/exit) of a hemispherical analyzer, electrons with energy 20 eV are detected by a channeltron. The instrumental resolution measured as the full width at a halfmaximum (fwhm) of the Ag3d5/2, photoelectron peak is about 1 eV. The energy scale is corrected to the C1s (peak maximum at 285 eV) for electrostatic sample charging. The fitting of the recorded XPS spectra was performed, using a symmetrical Gauss-Lorentzian curve fitting after Shirley-type subtraction of the background. Except scanning the steel surface after 7 days i.e. product layers formed on the steel electrodes in each relevant condition, four-times consecutive mechanical polishing of equal pressure and time duration was performed in depth of the layer in the vacuum chamber of the spectrometer. This technique was chosen to avoid influence on the chemistry of the formed layers, which would otherwise be relevant if Ar sputtering was used. The XPS measurements thus resulted in quali- and quantifying of the composition of the product layers in depth i.e. for each specimen, four in depth scan results were recorded.

4 Results and discussion

4.1 Electrochemical measurements

4.1.1 OCP evolution and polarization resistance

A general perception is that the evolution of open circuit potential (OCP) determines the time to corrosion initiation. For reinforced concrete, and alkaline medium as the here used CE, the steel surface is considered to be passive if OCP is equal or more anodic than -270 mV SCE. When chlorides (or other corrosion-inducing factors) are present, passivity is lost and localised corrosion initiated – OCP readings shift to more cathodic (more negative) values in this case. Figure 2 depicts OCP evolution for the control (non corroding) cases (dotted notation), Fig. 3 shows these values for the corroding cases. Additionally, Figs 2 and 3 depict the derived (via linear regression) polarization resistance values (Rp) (Rp in global terms corresponds to corrosion resistance). As can be observed, OCP values fall in the region of passivity and shift towards more noble potentials at the end of the test. These correspond to the gradual increase of Rp values, the highest being for the steel treated in "empty" vesicles containing CE. Since there is no corrosion accelerator in the medium for the control samples, only gradual passivation is expected rather than any pronounced effect of the Ca-rich inner

"core" of the Ca-containing vesicles. However, adsorption of both vesicle types on the steel surface and their incorporation in the passive layer could result in possible alterations in compactness and/or speed of layer formation. Obviously, barrier effects in terms of diffusion limitations from the adsorbed "empty" vesicles are relevant for specimen CEV, since OCP values are more cathodic, whereas *Rp* values are the highest. This does not necessarily mean a better corrosion resistant layer, but possibly limited oxygen access and hence locally impeded growth of a more inhomogeneous layer. In contrast, the CE and CEVC specimens exhibit similar *Rp* values.

Apparently the Ca-containing vesicles either act as "nucleation sites" on the steel surface, adsorb on active spots, or both and therefore do not result in diffusion limitations as in the case of CEV specimens.

For the corroding cases (Fig. 3), a shift to more active (cathodic) OCP values is as expected and as observed for specimens CEn (steel treated in vesicles-free solutions). This corresponds to the decreasing *Rp* values with time of treatment. In contrast, specimens CEVn and CEVCn depict OCP values in the passive range at the end of the test (more anodic than -200 mV) and higher *Rp* values. The influence of Ca-containing vesicles is here already well pronounced: after initially lower values, and even lowest after 4 days treatment, the *Rp* values for
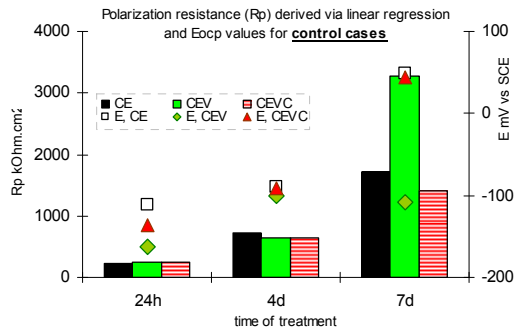

Figure 2:   OCP and *Rp* values for control cases.

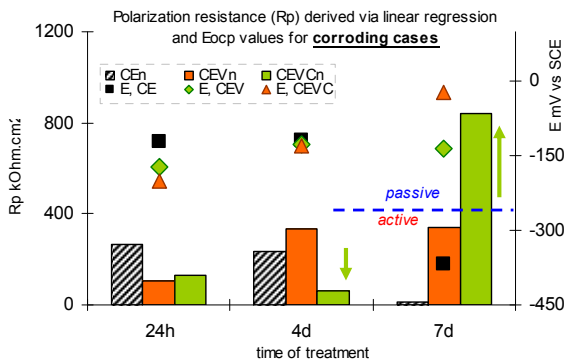
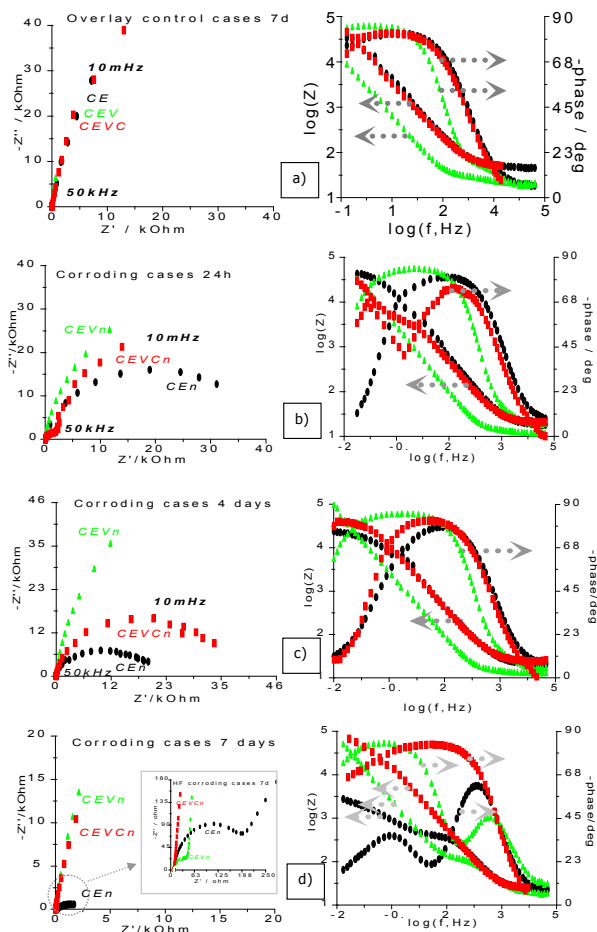
Figure 3:   OCP and *Rp* values for corroding cases.

Figure 4:   7d EIS response for CE, CEV and CEVC (a) and CEn, CEVn, CEVCn after 24h (b), 4d (c) and d (d).

specimens CEVCn depict a significant increase at the end of the test. Since the steel electrodes, treated in CE containing "empty" vesicles do not show this trend (specimens CEVn), the only plausible explanation is that the Ca-containing vesicles exert a "self-repair" or 'self-healing' of the already induced corrosion damage on later stages of treatment. These observations are actually confirmed by EIS, PDP and CVA tests and supported by surface analysis.

4.1.2 EIS, PDP and CVA results
The EIS response is not subject to elaborated discussion in this paper, but is presented as a direct visualisation of the electrochemical behaviour of the steel electrodes. Figure 4(a) presents the response for the control specimens after 7days. Figure 4(b)–(d) depicts the response of all corroding cases after 24h (b), 4d(c) and 7d (d) treatment. As seen from the plots, the magnitude of impedance

|Z| is higher for the steel treated in vesicles containing solutions at all time intervals, accompanied by a mostly constant phase angle of approx. 80°, whereas for the vesicles-free cases the phase angle drops to approx. 65° at the end of the test. The EIS results clearly show the "self-repair" of the product layer on the steel surface when Ca-containing vesicles are involved: specimens CEVCn depict a response with two time constants after 24h treatment, meaning a pronounced contribution of product layer alterations in parallel to charge transfer resistance phenomena. Later on, the magnitude of |Z| slightly drops, whereas the phase angle increases, which can only be denoted to modified product layer morphology and composition, rather than increase in charge transfer. Further, after 7 days treatment, both magnitude of |Z| and phase angle increase, denoted to improved and more corrosion resistant steel surface (one time constant only at 7d). The only barrier, rather than "self-healing" effect in specimens CEVn ("empty" vesicles involved) is seen from the gradual decrease of impedance and phase angle and pronounced contribution of a second time constant at the end of the test. These observations are in line with the electrochemical behaviour with external polarization – PDP and CVA response. Fig. 5(a) depicts PDP curves for all corroding cases as an overlay of 4d and 7d response; Fig. 5(b) presents the response of specimens CEVCn only for all time intervals.
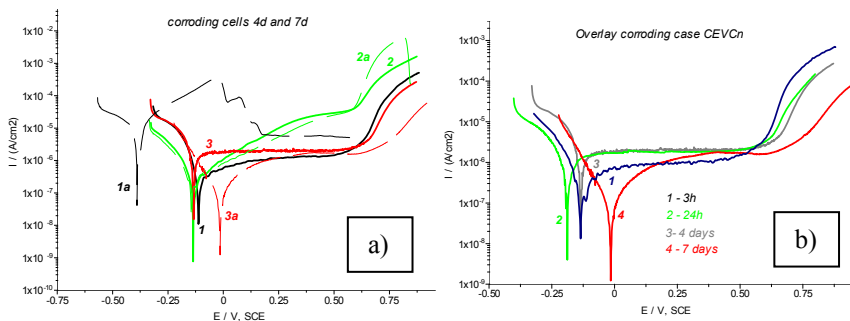

Figure 5:   (a) PDP curves for specimens: CEn at 4d and 7d (curves 1 and 1a); CEVn at 4d and 7d (curves 2 and 2a); CEVCn at 4d and 7d (curves 3 and 3a); (b) PDP response for specimen CEVCn at 3h, 24h, 4d and 7d (curves 1, 2, 3 and 4 respectively).

After 4 days treatment the corrosion current density for specimens CEn and CEVn are similar (curves 1 and 2, Fig. 5a)), the anodic current with external polarization for specimens CEVn is even higher than that for CE. This proves the previously discussed diffusion limitations in specimen CEVn and barrier effects of the "empty" vesicles, which do not result in a stable and homogeneous product layer, since anodic currents are not limited but increasing with polarization. Specimens CEVCn present slightly higher corrosion current density, but a significant anodic limitation with external polarization is relevant (curve 3, Fig. 5a). The latter observation is in line with the previously discussed attempts to "repair" of initially induced corrosion damage. After 7d treatment,

the CEn specimens (curve 1a, Fig. 5a) exhibit the highest anodic and corrosion currents (as expected) and significant shift of corrosion potentials to more cathodic values. In contrast, specimens CEVCn (curve 3a, Fig. 5a) present a drop of corrosion and anodic current densities, a shift to more noble corrosion potentials and maintained anodic currents limitations.

After 7d treatment, specimens CEVn present similar to the 4d behaviour of active dissolution with external polarization (curves 2a and 2, Fig. 5a). The self-healing effect of the "Ca-containing" vesicles, present in the medium of CE+ NaCl are well seen if a comparison is made of the response for specimens CEVCn with time – Fig. 5(b): after initially low currents (curve 1, 3h), corrosion is initiated (curve 2, 24h); the process is maintained until 4days, where slightly higher corrosion current is recorded, most likely corresponding to product layer transformations and Ca-content release and/or nucleation sites effect due to the "Ca-containing" vesicles on the steel surface. The result with prolonged treatment is product layer "repair", evident by a significant drop of corrosion and anodic currents (curve 4, 7d) and further anodic limitations.
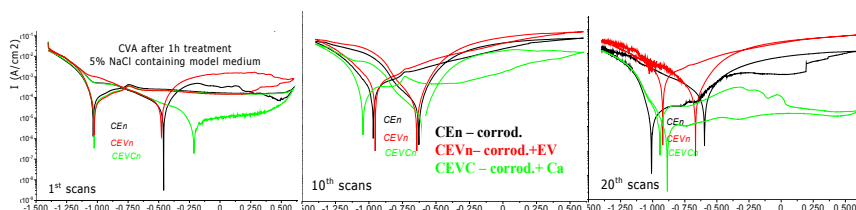

Figure 6:   CVA scans for specimens CEn, CEVn and CEVCn

CVA tests strongly support all above observations. Fig. 6 presents the 1st, 10th and 20th scans, recorded after treatment in the relevant solutions. As seen from the plots, pitting initiates for specimens CEn and CEVn (at approx. -325 mV) with the 1st scan, whereas no pitting was observed for specimens CEVCn, the latter exhibiting the lowest current densities in the reverse scan and most noble re-passivation potential (Fig. 6). After 10 scans, all specimens, including CEVCn show pitting formation at around -500 mV (Fig. 6) and shift towards higher currents in both anodic and cathodic sweeps. Finally, within 20 scans (Fig. 6) the self-healing effect of the Ca-containing vesicles is evident from the recorded significantly low currents for specimens CEVCn in both anodic and cathodic sweeps, accompanied by the lack of pitting formation. In contrast, for specimens CEn and CEVn, pitting propagation is still relevant, accompanied by already largely increased currents in both anodic and cathodic sweeps.

4.2 Surface analysis

The previously discussed possible characteristics of the formed on the steel surface product layers with respect to electrochemical response were actually as observed via ESEM, EDX and XPS analysis. Fig. 7 presents ESEM micrographs and the relevant EDX analysis for the corroding cases (b-d); for a comparison,
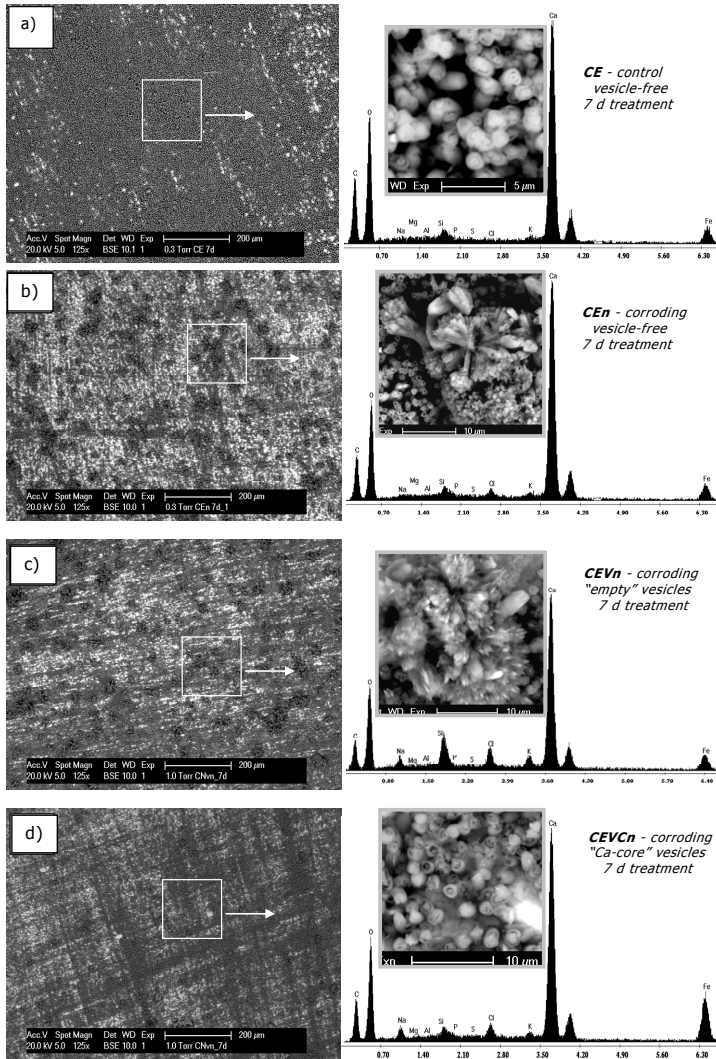
Figure 7: ESEM micrographs and the relevant EDX analysis for control (a) and corroding cases CEn (b), CEVn (c) and CEVCn (d).

the control case (CE) is depicted in Fig. 7a) (the layers at higher magnification are given as inlets in the EDX patterns).

As seen from Fig. 7 the morphology and composition of the product layer for corroding specimen CEVCn (Fig. 7d) resembles the one observed for the control specimen CE (Fig. 7a) i.e. a more compact layer, depicting mainly calcium carbonate was observed. Should be noted that for all specimens, $CaCO_3$ was detected by both ESEM/EDX and XPS (Fig. 8) (the XPS and ESEM/EDX investigations were performed after removing the specimens from the model

solutions and drying on air). Since the specimens were in immersed condition, carbonation of the solutions during treatment is minimal. Moreover, if a substantial concentration of CO_2 in the solutions was present, $FeCO_3$ will form, which would be either detected by XPS and ESEM, or would rather rapidly transform when the specimens are taken on air to more stable iron oxides ($FeCO_3$ or "green rust" is not stable in oxygen containing environment). Therefore, the detected surface $CaCO_3$ is a result of the reaction of Ca-containing compounds (as CaO and $Ca(OH)_2$ previously deposited on the steel surface during treatment) with atm. CO_2 upon drying of the specimens on air. Consequently, the presence and amounts of $CaCO_3$ on the steel surface can serve as an indirect indication for the presence of adhered Ca-containing compounds during treatment in immersed condition. To this end, the control cases and specimens CEVCn present mainly carbonate-rich product layers, whereas for specimens CEn and CEVn (Fig. 7(b), (c) except $CaCO_3$, chloride-containing iron oxides/hydroxides are relevant. This is in line with the lower corrosion resistance, detected via electrochemical measurements. In specimens CEn and CEVn localised corrosion is basically observed, evidenced by the deposition of voluminous, needle-shape corrosion products (Figs. 7(b),(c).)
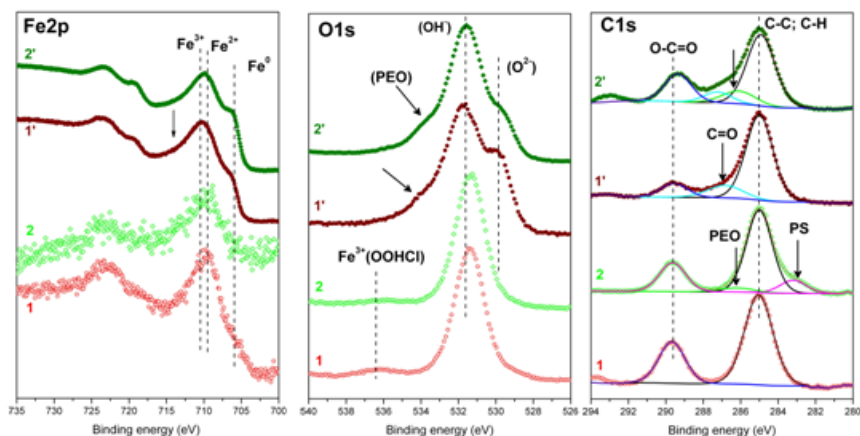

Figure 8: XPS iron (Fe2p), oxygen (O1s) and carbon (C1s) ionization for specimens CEn (curves 1 and 1') and CEVCn (curves 2 and 2').

An elaborated discussion on the otherwise extensive XPS analysis is not subject to this paper and will be separately reported. What needs to be mentioned are only main observations and features, supporting the above results and discussion.

As previously defined, XPS was performed on the surface of the as-treated specimens (after 7 days) and in depth of the (7 days-old) product layers. Fig. 8 presents the ionizations of Fe, O and C on the "as-treated" surface (scans 1 and 2) and in depth of the products (scans 1' and 2'). With respect to iron oxides and hydroxides, all specimens exhibit a mixture of these with a larger portion of the

latter in the outermost sections of the layers (shape and features of the scans 1 and 2 in Fe2p, pronounced peak at 531.6 eV in O1s, corresponding to OH⁻) and a larger portion of the former (oxides) in depth of the layers (hematite/magnetite based layers as evident from the characteristic features of Fe2p, 1' and 2' and the peaks at lower binding energy ~ 529 eV in the O1s for 1' and 2'). As also observed, metallic iron appears in dept of the layers as well (~706 eV), which is as expected within product layer removal. The presence of adsorbed in the product layers vesicles for specimen CEVCn is confirmed by the characteristic binding energies in the C1s ionizations i.e. 283 eV for PS, 286.5 eV for PEO and 534 eV for PEO in the O1s ionizations. Iron oxy/hydroxy chlorides are detected only in the outermost layers for (mainly) specimens CEn (peak at 536.1 eV in O1s), which is actually supported by the morphological observations on the surface of CEn (Fig. 7b). In other words, morphological and chemical alterations in the product layers, formed on the steel surface in the presence of Ca-containing vesicles and chloride result in a "self-repair" or "self-healing", evidenced by a more compact and uniform product layer, featuring iron oxy/hydroxides and calcium carbonate only (similar to the layers, formed in the control, chloride-free cases). In contrast, for steel treated in vesicles-free or "empty" vesicles containing solutions, voluminous iron-oxy/hydroxy chlorides and lower amount of Ca-containing compounds are present.

5   Conclusions

In the frame of a novel approach to corrosion control in reinforced concrete, the application of polymeric nano-particles was investigated. In order to evaluate the difference between "barrier" effects only and self-healing mechanisms, resulting from the "Ca-core" release, the effect of both "empty" and Ca-containing vesicles was studied. In the presence of both vesicle types corrosion resistance was increased, but the effect was significantly more pronounced when Ca-containing vesicles were involved. The concentration of 0.0024 wt.% vesicles in the model solutions is minimal and therefore self-repair or self-healing of the product layer solely due to the Ca-component is not realistic. The most plausible mechanism is the nature of incorporation of the Ca-containing vesicles in the product layer, enhanced chloride binding effects and adsorption on active sites on the steel surface. The result is a more uniform and stable steel surface layer, initial pitting formation and propagation, but consecutive healing, as evidenced by surface analysis and electrochemical response i.e. largely reduced anodic and corrosion currents and no further pit propagation when Ca-containing vesicles are present.

References

[1]   Conway, BE, Theory and principles of electrode processes, 170-272, The Ronald Press Company, NY (1965)
[2]   Broomfield J (1997) Corrosion of steel in concrete, understanding, investigating and repair. Spon, London

[3]   Sahmaran M (2007) J Mater Sci 42:9131. doi:10.1007/s 10853-007-1932-z
[4]   Elsener B (2002) Cem Concr Compos 24(1):65
[5]   Garces A, Andrade MC, Saez A, Alonso MC (2005) Corros Sci 47(2):289
[6]   Uhlig HH (2000) In: Revie RW (ed) Uhlig's corrosion handbook., p 583
[7]   Bertolini L, Elsener B, Pedeferri P, Polder R (2004) Corrosion of steel in concrete: prevention, diagnosis, repair, 1st edn. Wiley, Weinheim
[8]   Petterson K (1994) In: Swamy RN (ed) Corrosion and corrosion protection of steel in concrete. Academic Press, Sheffield, p 461
[9]   Pedeferri P, Constr. Build. Mater., 10, 391 (1996)
[10]   Bassi R., Davies H, Testing anti-carbonation coatings for concrete, BRE Information paper IP7/96, 1996
[11]   Buenfeld N. Buenfeld, J.Z. Zhang, Cem. Concr. Res. 28 (1998) 665-674
[12]   Castle J.E., Cathodic disbondment, Proceedings of the AIP Conference p. 165, (1996)
[13]   Bird C.E, Nature, 194:798 (1962)
[14]   Herrera MJ, Martinez M and Perez JT, Evaluation of Electrochemical behavior of Two Inhibitors for Galvanized Rebars in Alkaline Solutions, paper 831, 210th meeting ECS, Cancun, MX (2006)
[15]   Intern. Lead Zinc Research Organisation. Galvanized reinforcement for concrete II. Res. Triangle Park NC, USA, 1981
[16]   Obada K, Stephen R. Yeomans, Cem.Concr.Comp.22, 459-467, (2000)
[17]   Andrade C, Holst JD. Coating protection for reinforcement. Comite Euro-International Du Beton. State of the Art Report. London: Thomas Telford Publication; 1995. p. 51
[18]   Mietz J, Electrochemical Rehabilitation Methods for Reinforced Concrete Structures: A State of the Art Report, in, Institute of Materials, 1 Carlton House Terrace, SW 1 Y 5 DB, London, UK, 1998
[19]   Andrade C., Keddam M, Nóvoa X. R., Pérez M. C., Rangel C. M., Takenouti H., Electrochim. Acta, 46, 3905-3912 (2001).
[20]   Gaidis M., Cement and Concrete Composites, 26 (2004) 181-189
[21]   Wombacher F., Maeder U., Cem. Concr. Comp., 26 (2004) 209-216
[22]   Koleva D.A., van Breugel K., Ye G., Koenders E., ACI Mater. J. 267 (2009)101-110
[23]   Koleva D.A., Jie Hu, Van Breugel K., J. Intern. Sci. Publ.: MMT5 (2011) 63
[24]   Hu J., Koleva D.A., Petrov P., van Breugel K., Corr. Sci. 65 (2012) 414-430
[25]   Hu J., Koleva D.A., Ma Y., Schlangen E., Petrov P., van Breugel K., Cem. Concr. Res. 42 (2012) 1122-1133
[26]   Hu J., Koleva D.A., van Breugel K., J. Mater. Sci. 47 (2012) 4981-4995
[27]   Hu J., Koleva D.A., et. al. J. Electrochem. Soc. 158 (2011) C76
[28]   Hu J., Koleva D.A., van Breugel K. ECS Transactions, 41 (16) 1-9 (2012)